Journal of Physics: Conference Series **498** (2014) 012009 doi:10.1088/1742-6596/498/1/012009

ATHENA 3D: A finite element code for ultrasonic wave propagation

C Rose[1], F Rupin[2], T Fouquet[1], B Chassignole[2]
[1]EDF R&D SINETICS, Clamart (92), France
[2]EDF – R&D MMC, Sites des Renardières, Moret sur Loing (77) France

E-mail : Christian.rose@edf.fr

Abstract. The understanding of wave propagation phenomena requires use of robust numerical models. 3D finite element (FE) models are generally prohibitively time consuming. However, advances in computing processor speed and memory allow them to be more and more competitive. In this context, EDF R&D developed the 3D version of the well-validated FE code ATHENA2D. The code is dedicated to the simulation of wave propagation in all kinds of elastic media and in particular, heterogeneous and anisotropic materials like welds. It is based on solving elastodynamic equations in the calculation zone expressed in terms of stress and particle velocities. The particularity of the code relies on the fact that the discretization of the calculation domain uses a Cartesian regular 3D mesh while the defect of complex geometry can be described using a separate (2D) mesh using the fictitious domains method. This allows combining the rapidity of regular meshes computation with the capability of modelling arbitrary shaped defects. Furthermore, the calculation domain is discretized with a quasi-explicit time evolution scheme. Thereby only local linear systems of small size have to be solved. The final step to reduce the computation time relies on the fact that ATHENA3D has been parallelized and adapted to the use of HPC resources. In this paper, the validation of the 3D FE model is discussed. A cross-validation of ATHENA 3D and CIVA is proposed for several inspection configurations. The performances in terms of calculation time are also presented in the cases of both local computer and computation cluster use.

1. Introduction

For obvious safety reasons, maintenance and In-service inspection is of great importance for nuclear power plants operators like EDF. Ultrasonic techniques are in particular very useful to detect and size potential flaws localized in depth in the metallic components. In these techniques, the detection is mostly based on amplitude criterion of the reflected signal from the defect. But, in some cases, due to unfavorable wave to microstructure interaction, the performances of the control can decrease significantly [1, 2]. Furthermore, the use of one NDT method for onsite nuclear inspection is conditioned by a qualification procedure which has to demonstrate the performances of the chosen technique. In this context, modeling codes can be of a great interest since they allow parametric studies [3] and avoid providing expensive mock-up. However, a good accuracy of the numerical results necessitates the taking into account of all physical phenomena involved in the wave propagation in polycrystalline media. In particular Finite Element (FE) codes have proved their efficiency to accurately reproduce complex phenomena such as beam deviation, division or attenuation [4-7]. During the past decade, EDF R&D developed in collaboration with INRIA the FE code ATHENA2D dedicated to the solving of the elastodynamics equations in all kind of elastic media [4, 8-10]. This code has already been widely used in order to simulate complex inspection configurations and is consequently relatively well documented. Nevertheless, up to now, only the 2D version of the code was available since an important amount of inspection configurations can be approximated by 2D models and 3D finite element (FE) models were generally considered to be prohibitively time consuming. But, in some cases, 3D simulations are required. However, the advances in computing

processor speed and memory allow them to be more and more competitive and lead EDF R&D to develop the 3D version of the ATHENA code.

In this paper, the main characteristics of the code as well as the chosen numerical scheme are described. The performances in terms of calculation time are also presented in the cases of both local computer and calculation cluster use. We then present some cross-code validation configurations between the FE code ATHENA and the semi-analytical code CIVA. **2. Mathematical model**

ATHENA is a finite element code that simulates wave propagation in all kind of elastic media by solving the elastodynamic equations expressed in a mixed formulation combining stress and velocity terms (σ and v respectively).

Equations (1) and (2) are solved on a 2D or 3D calculation domain Ω whose boundary is ∂Ω and respects condition (3). Furthermore, a defect Γ can be included inside Ω as long as the free surface boundary condition (4) is satisfied. The particularity of the code relies on the fact that the interaction between the beam and the defect is simulated using the fictitious domains method. In this case, the defect is discretized with a triangular mesh (in the 3D case, with segments in the 2D case) independent of the 3D Cartesian mesh of Ω and allows arbitrary shape and orientation of the defect [11, 12].

(1) $\rho\, \partial v/\partial t - \mathrm{div}\sigma = f$,
(2) $A\, \partial\sigma/\partial t - \varepsilon(v) = 0$ on Ω,

(3) $\sigma.n = 0$ on $\partial\Omega$
(4) $\sigma.n = 0$ on Γ

where, v is the velocity in Ω, σ is the stress tensor, $\varepsilon_{i,j}(v) = \frac{1}{2}(v_{i,j} + v_{j,i})$, $A = C^{-1,}$ with C the elasticity tensor and ρ is the density.

In addition, ATHENA gives the possibility to use perfectly matched absorbing layers (PML) to define the boundaries of the calculation domain in order to avoid parasite reflections on the artificial edges of the calculation zone and allow simulation in infinite domains.

3. Numerical Scheme

The discretization of (1) and (2) using of an appropriate variational formulation leads to the following numerical scheme:

$$(5)\ M_v \frac{V^{n+1} - V^n}{dt} + B\ \sigma^{n+1/2} = F^{n+1/2}$$

$$(6)\ M_s. \frac{\sigma^{n+1/2} - \sigma^{n-1/2}}{dt} + B^T.V^n - D^T.\Lambda^n = 0.$$

$$(7)\ \ D.\ M_s^{-1}.D^T.\Lambda^n = D.\ M_s^{-1}\ B^T\ .V^n$$

The notation V^n is used to represent V at time step n*dt. The above-written equations introduce a new quantity Λ, which is a Lagrange multiplier used to ensure the boundary condition (4). Mass matrices M_v and M_s depend respectively on the quantities ρ and A seen above and are block diagonal making the numerical scheme quasi-explicit. Matrix B is a discrete divergence operator and D is "trace operator" of the defect mesh on the domain mesh. Concerning the time discretization, we can notice that σ and V are not computed at the same time, (5) and (6) belongs to the class of "leap-frog" schemes.

4. Space discretization

The calculation domain Ω where equations (5) to (7) are solved is limited to rectangular surfaces in the 2D case and to rectangular parallelepipeds in the 3D case so that a regular Cartesian mesh is used for the discretization. The computation of V is performed in the middle of the cells (plane-rectangular or

cubes) while σ is calculated at the nodes. However we do not compute one value of σ at each node. The choice of the finite elements leads to discontinuities at each cell for the different components of tensor σ. Indeed if we consider the 3D case: on one hand, σ_{xy} is continuous in both directions x and y, and discontinuous in direction z. On the other hand σ_{zz} is only continuous in direction z. So we have to compute 18 stress degrees of freedom on each node. We only have to solve a small system of 18 equations on each node, which is less time consuming than a global implicit system which would be a 21*Nx*Ny*Nz matrix.

As the mesh is regular, the stability of the explicit scheme can be easily ensured with $h = V_p * dt$, with V_p being the longitudinal velocity, dt the time step and h the mesh size.

The additional unknowns Λ, introduced by the fictitious domains method on every nodes of the defect mesh, can be obtained by solving a linear system at each time step. The order of the corresponding matrix is the number N of nodes of the defect mesh. Furthermore this matrix is constant and factorized once before the transient calculus.

5. Parallelization

Even if ATHENA does not deal with a global linear system of equations, the computation time of 3D configurations can become prohibitive in a local computer. In order to increase the competiveness of the code, it has been parallelized using the send/receive mechanism of the well-documented MPI (Message Passing Interface) library. In the parallelized version of ATHENA, the domain Ω is divided along Z axis in np chunks of size Nz/np, where np is the number of processors used. Two processors, in charge of two subdomains, can then communicate, sending and receiving data belonging to their common boundary (Figure 1). Furthermore, one can notice that there is no limitation for the defect due to parallelization since the defect can belong to more than one subdomain.

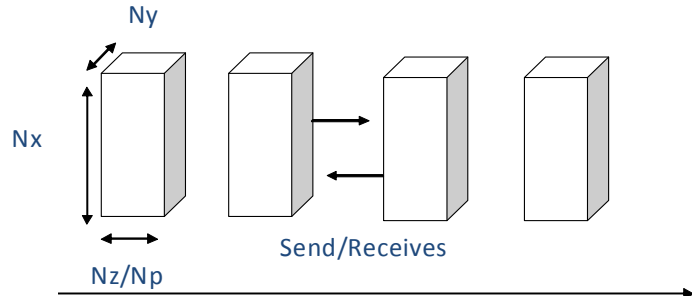

Figure 1. Communication scheme of two processors in Athena3d parallelization.

6. Computation time performances

According to the sizes of problems, ATHENA3D can be run on different kinds of computers. Small size problems can run on local machines. Indeed the development of multi-cores processors gives the possibility to take advantage of parallelization with 8 or 12 processors on local computers. However, for bigger size problems, the use of a calculation cluster becomes necessary. Table 1 summarized the computing times obtained on different machines for three different test cases with regard to their main numerical characteristics (number of cells, number of time steps and mesh size). However, it only gives an assessment of computing resources needed, and are not “best effort” performance times obtained by optimization.

The test cases are the followings:

- Case 1 corresponds to the inspection of a 10mm high notch located at 20 mm depth in stainless steel with a 0.2 mm mesh size
- Case 2 corresponds to the inspection of a 0.6 mm diameter SDH located at 30 mm depth in stainless steel and a mesh size of 0.08mm.
- Case 3 is similar to case 2 but with a 0.04mm mesh size

The local computer used for the time performances evaluation includes two Intel processors (Nehalem type, frequency: 2.3 GHz), with 12 Gbytes of memory. Eight cores are then available on this computer.

The cluster used in this study contained about 2000 computing nodes. Each node includes two Intel "Westmere" processors (frequency: 2.8 GHz), providing 12 cores and exhibits 24 Gbytes of memory. On such a node parallel computing can be run with 12 processes on 12 cores.

Table 1. Different calculation times of ATHENA3D

	Number of cells	Number of time step	Mesh size (mm)	Time calculation Local computer	Time calculation cluster
Case1	$4\ 10^6$	735	0.2	20 minutes	-
Case2	$75\ 10^6$	3215	0.08	~18 H	9 Hours
Case3	$200\ 10^6$	5700	0.04	-	30 H

The mesh size of case 1 is 0.2 mm which is a common value for 2 MHz longitudinal wave. As a consequence, the number of cells is limited enough to allow a local calculation of the inspection configuration. In this study, Case 1 was calculated using the 8 cores available on the local machine.

For Case 2, the use of the calculation cluster decreases the computation time by a factor of two. However, the calculation was launched on only one node of the cluster, so the 9 hours of computing time were obtained with a limited 12 cores parallelization. It means that the computation could have been run on a bigger amount of cores implying a decrease of the computing time.

Case 3 needed a big amount of memory such as the calculation could not be run on a local machine. Furthermore, for the cluster calculation, the domain Ω had to be divided into 24 subdomains, each one needing an entire computing node, and, as a result, used only one of the 12 cores. This is a "memory driven" case. Finally a 200 million cells calculation has been calculated in 30h.

Nevertheless, it has to be noted that the computation time performances were evaluated for a configuration with only one Ascan, i.e. one position of the UT probe. When an entire Bscan must be simulated, the use of the calculation cluster allows a more than substantial gain of time since each Ascan can be launched simultaneously while they have to be calculated sequentially in a local machine.

7. Athena pre/post processing

The utilization of ATHENA is simplified by the integrated Graphical User Interface (GUI): MILENAQt (Figure 2). It helps the user to create the simulation configuration, i.e. the calculation domain, defect shape and size, probe characteristics, etc., through the existence of various menus and submenus guiding the user step by step. Furthermore, it includes a preprocessing stage consisting in an automatic meshing of the defect and calculation domain and the computation of the source field using the probe characteristics defined by the user. Finally, MILENAQt integrates the post-processing and the visualization of the results (Figure 3).

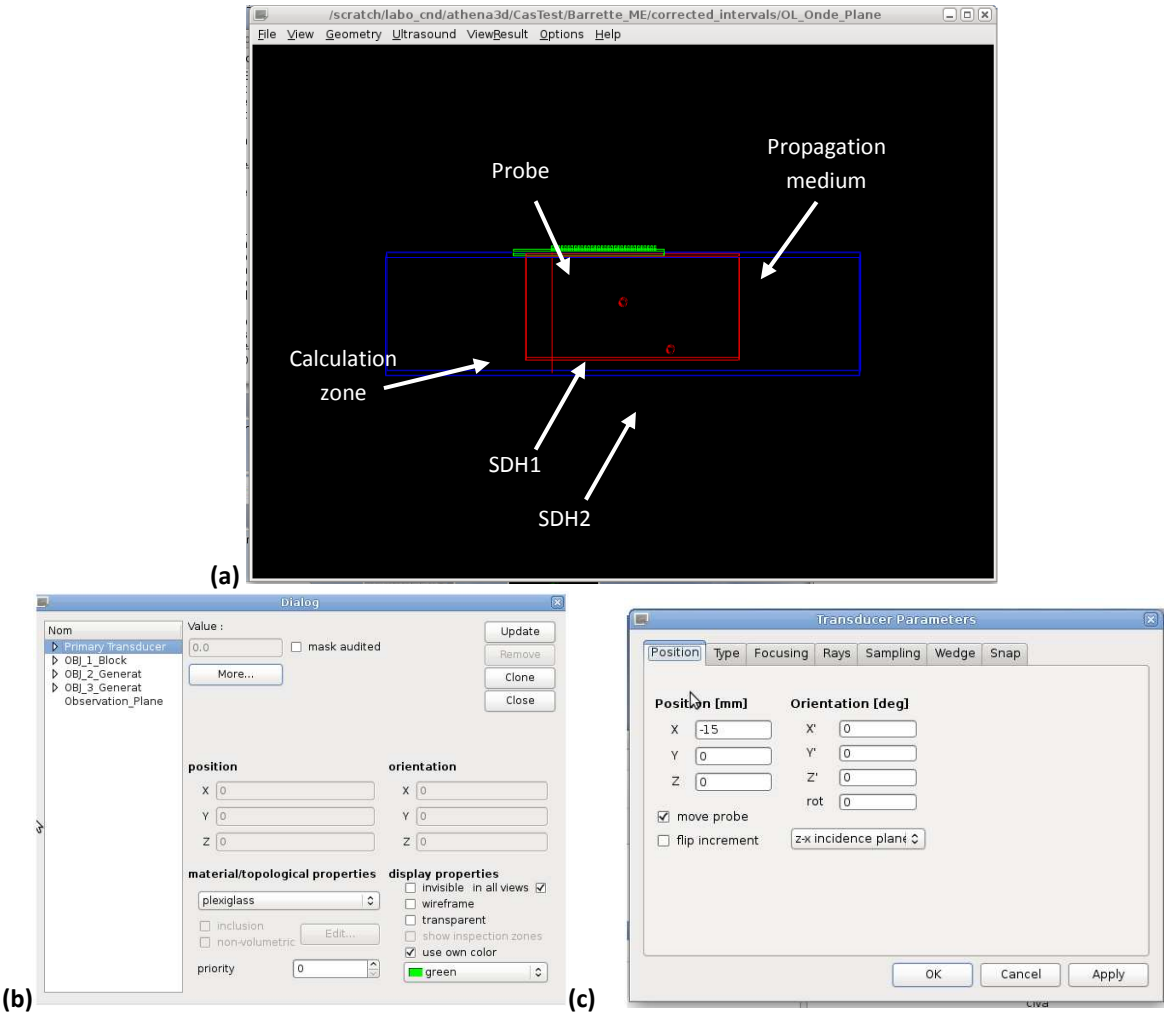

Figure 2. Illustration of the GUI MilenaQt. (a) shows the visualization of the inspection configuration: two SDH and a linear phased array probe. (b) shows the dialog box dedicated to the definition of the inspected object (propagation media and defects). (c) shows the dialog box dedicated to definition of the transducer parameters.

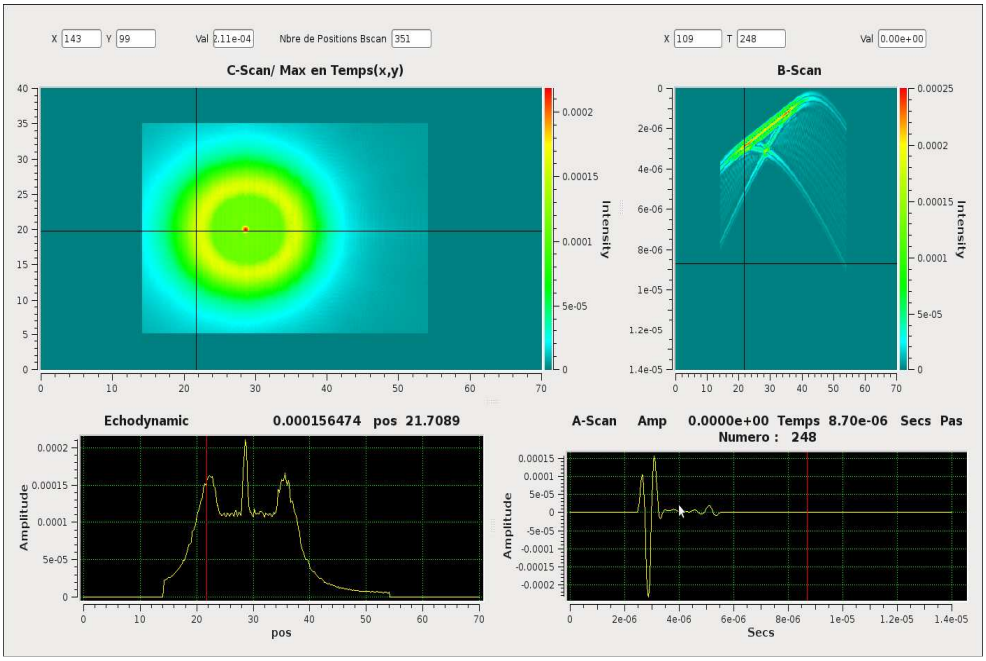

Figure 3. Example of beam visualization with MilenaQt.

8. Test configurations in a homogeneous and isotropic medium

In this study, three validation cases were scrutinized. In each case, the propagation medium made of austenitic stainless steel is isotropic and homogeneous (V_L= 5 700 m/s, V_S= 3130 m/s and its density is d=7.9).

The first configuration involved the detection of two side drilled holes (SDH) located at 10 and 20 mm depth with a 1.5 mm diameter. Four different single element 2MHz probes were simulated. Their characteristics are summarized in Table 2. An example of configuration is given Figure 4.

The amplitudes of the SDH echoes obtained with ATHENA3D were compared with the ones derived from CIVA10 simulations performed with the same inspection description. The results are summarized in Table 3. The amplitude of the 10 mm depth SDH was used as the reference.

Table 3 shows a good agreement between the two codes. Indeed, except for the fL55 law for whom the discrepancy is 1.5 dB, the differences between ATHENA3D and CIVA 10 are inferior to 0.5 dB. Furthermore, the focalization effects are correctly taking into account such as the amplitude of the 20 mm depth increases significantly when using the appropriate focal law (fL0 case). In addition, Figure 5 shows the fields obtained for the two focalized probes for both ATHENA3D and CIVA 10. They exhibit very similar properties and in particular, they provide the same focusing depths.

Table 2. Characteristics of the probes used for the first validation case

Probe	Element shape	Propagation angle in austenitic steel (°)	Inspection type
L0	Cylindrical R= 6mm	0	Contact (wedge 5mm high) Plane L wave
L55	Cylindrical R= 6mm	55	Contact (wedge 15mm high) Plane L wave
fL0	Spherical Curvature radius = 150 mm R= 20 mm	0	Immersion (water height =50 mm) Focused L wave (focalization depth = 22 mm)
fL55	Spherical Curvature radius = 150 mm R= 20 mm	55	Immersion (water height =50 mm) Focused L wave (focalization depth = 12 mm)

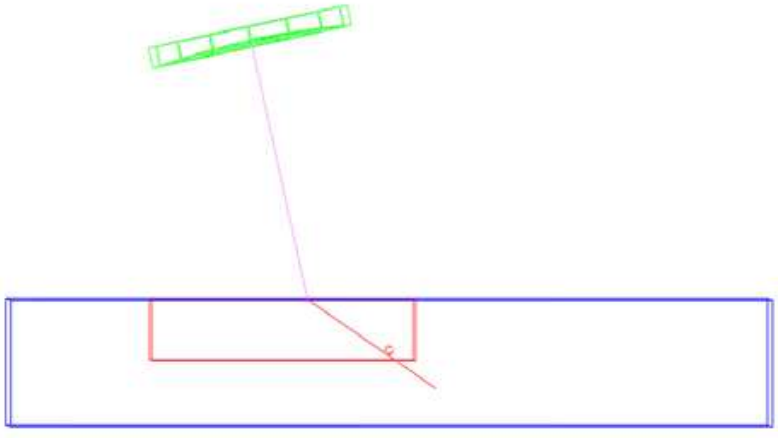

Figure 4. Inspection configuration of a 1.5 mm diameter of SDH located at 10 mm depth with a focused mono-element probe at the propagation angle of 55°.

Table 3. Amplitudes of the 20 mm depth SDH echo normalized by the 10 mm depth SDH obtained with ATHENA3D and CIVA 10

	L0 (dB)	L55 (dB)	fL0 (dB)	fL55 (dB)
ATHENA3D	-1.5	-6.0	+15.0	-4.0
CIVA 10	-1.5	-6.0	+15.5	-2.5

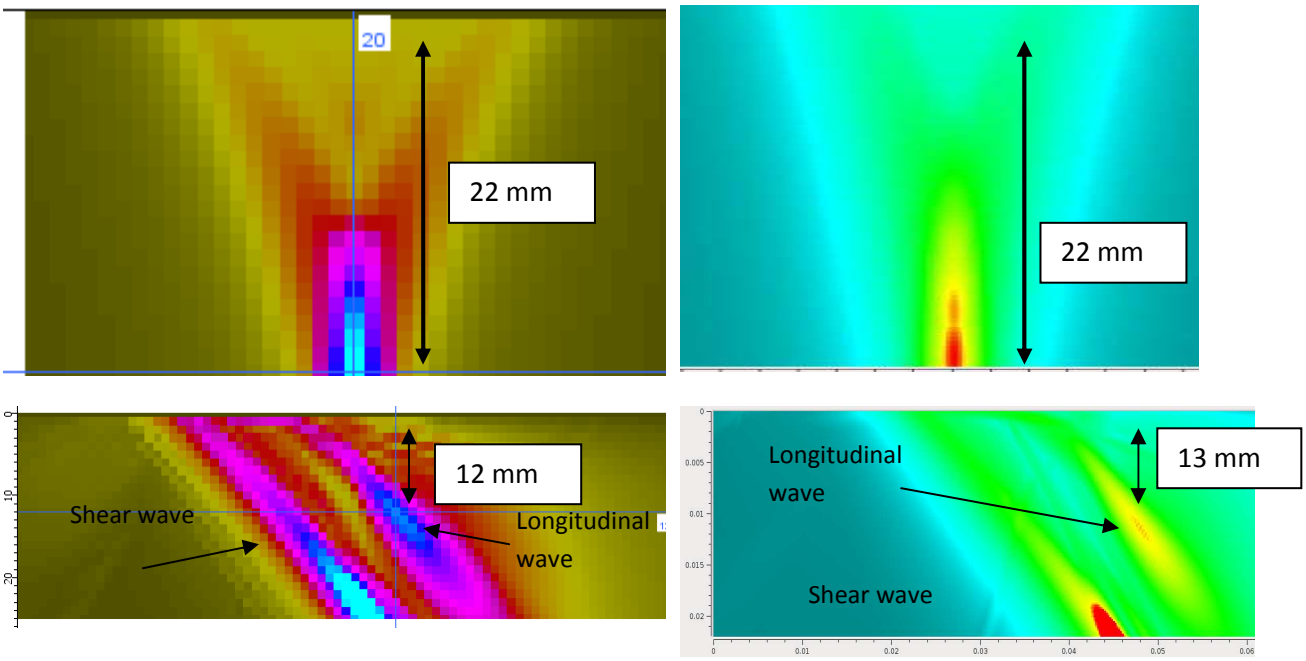

Figure 5. Sound field for the fL0 and fL55 calculated using CIVA 10 (left) and ATHENA3D (right).

The second configuration corresponds to the detection of a 10 mm height notch with a TRL55 probe (separate transmitter/receiver probe, longitudinal wave at 55° of incidence and 2MHz central frequency). The inspection configuration is given Figure 6. The Bscan obtained using ATHENA3D (25 scans with 1 mm step) can be observed on Figure 7. The main expected phenomena are clearly visible: the diffraction, the corner and the LLT mode conversion echoes are present. As for the previous configuration, the amplitudes of these echoes were compared to those computed using CIVA10. The results are summarized in Table 4. Again, a good agreement between CIVA and ATHENA was observed since the discrepancy between the two models is inferior to 2 dB.

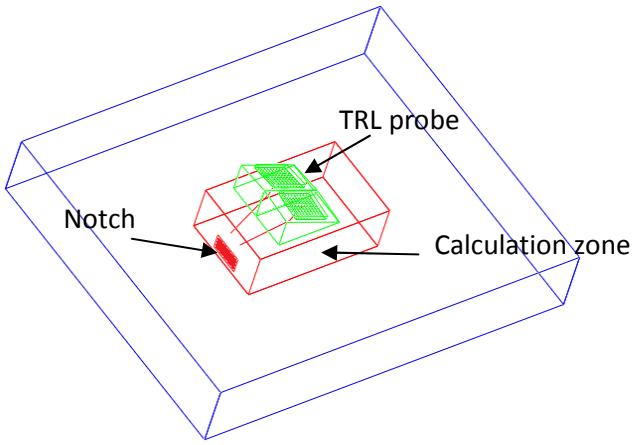

Figure 6. Inspection of a 20 mm high notch with a TRL probe (incidence angle of 55°)

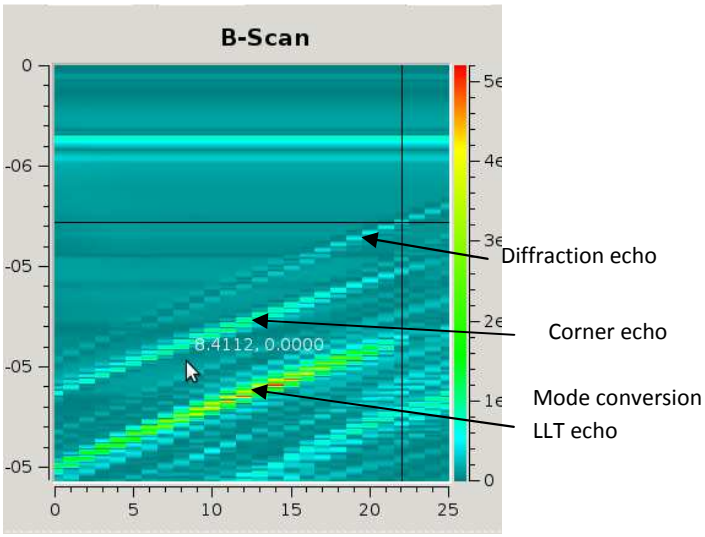

Figure 7. Bscan corresponding to the inspection of a notch with a TRL probe. The diffraction, corner and mode conversion echoes are clearly visible.

Table 4. Amplitude of the main echoes coming from the notch inspection. The reference is a 1.5 mm diameter SDH located at a 30 mm depth

	Corner (dB)	Diffraction (dB)	LLT (dB)
ATHENA3D	3.0	-6.0	13.5
CIVA 10	2.5	-8.0	11.5

The third configuration concerns the use of a linear phased array (PA) probe for the detection of 1.5 mm diameter SDHs. A 32 elements linear probe is simulated. Its properties are described in Table 5. The inspection configuration is illustrated Figure 8. Three focal laws were tested: L0 plane wave, L0 with a 10 mm focusing depth (0F10) and L0 with a 20 mm focusing depth (0F20).

Table 5. Properties of the simulated linear phased array

Central frequency	Element size	Array pitch	Number of element
2 MHz	0.3x15 mm²	0.5 mm	32

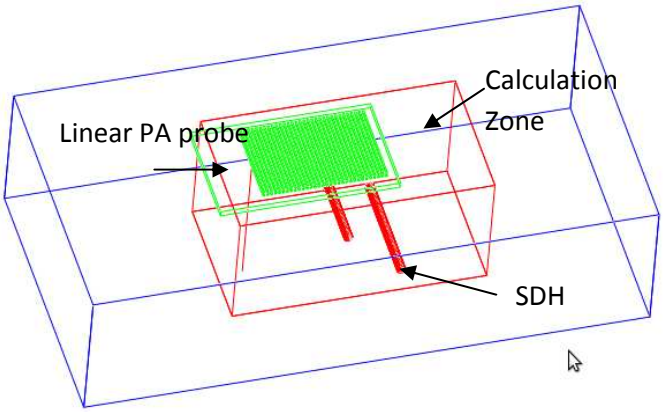

Figure 8. Inspection configuration of 2 SDH using a linear PA probe

The sound fields simulated for the 0F10 and 0F20 laws using CIVA 10 and ATHENA are given Figure 9 and Figure 10. In both cases, the focal laws are clearly taken into account. Furthermore, the two codes give similar results in terms of focal depth.

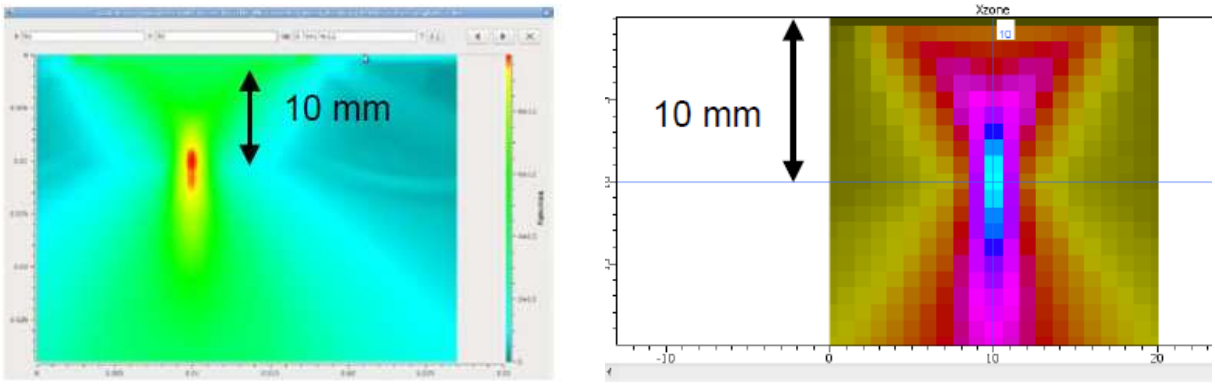

Figure 9. Sound field calculated using ATHENA3D (left) and CIVA 10 (right) for the 0F10 focal law

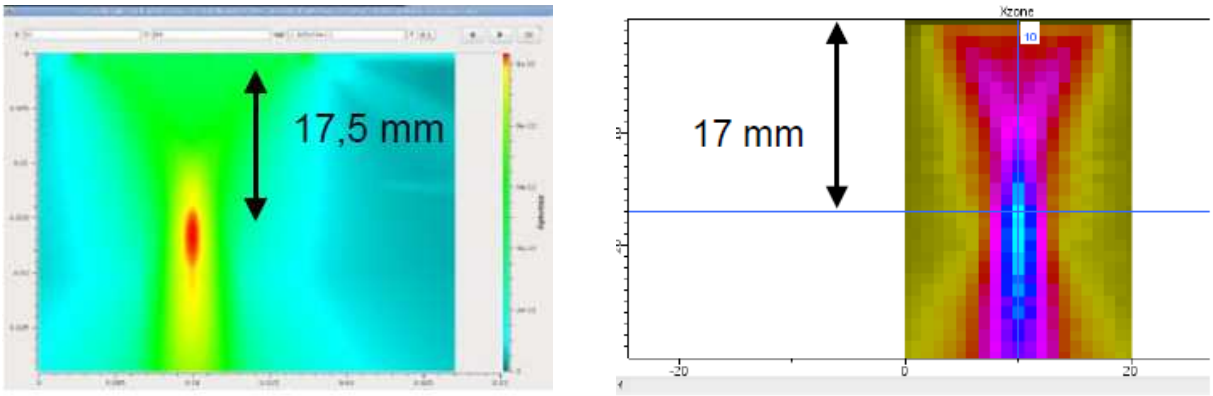

Figure 10. Sound field calculated using ATHENA3D (left) and CIVA 10 (right) for the 0F20 focal law

Concerning the detection of the SDHs, the amplitude of the 20 mm depth SDH obtained for the 3 focal laws and the 2 codes are summarized in Table 6. The discrepancy between the two remains inferior to 2 dB which is a satisfactory result in terms of cross-code validation.

Table 6. Amplitude (dB) of the SDH located at 20 mm depth. The reference is the amplitude of the 10 mm depth SDH measured with the focal law 0F10.

	Plane Wave	0F10	0F20
ATHENA 3D	-10.0	-7.5	-1.5
CIVA 10	-11.5	-8.5	-3.5

9. Anisotropic medium

A preliminary test has been realized to verify the capacity of the ATHENA3D code to take into account beam deviation when it propagates in an anisotropic (but homogeneous) medium. In this configuration, the simulated medium exhibits a density of 7 and transversally isotropic elastic properties (Table 7) and the probe provides a longitudinal wave with no incidence angle (L0). We want to evaluate the influence of the orientation of the principal symmetry axis on the beam propagation. To do so, three different cases are tested. In the first one, the symmetry axis is parallel to the propagation axis (z). In the second case, the symmetry axis undergoes a 15° rotation around the y-axis. In the third case, the symmetry axis is rotated by 15° around the x-axis (Figure 11).

For the three cases, the simulated sound field on an observation plane located at a 30 mm depth from the entry surface is given in Figure 12. The results are in very good agreement with the theory of ultrasound propagation in anisotropic media. Indeed, in the first case, no deviation is observed while in the second and third cases, an 8.5 mm deviation along the x axis and y axis (respectively) appears.

Table 7. Elastic properties of the transversally isotropic austenitic stainless steel used for the simulation

C_{11}	C_{22}	C_{33}	C_{44}	C_{55}	C_{66}	C_{12}	C_{13}	C_{23}
247	247	218	105	105	80	105	148	148

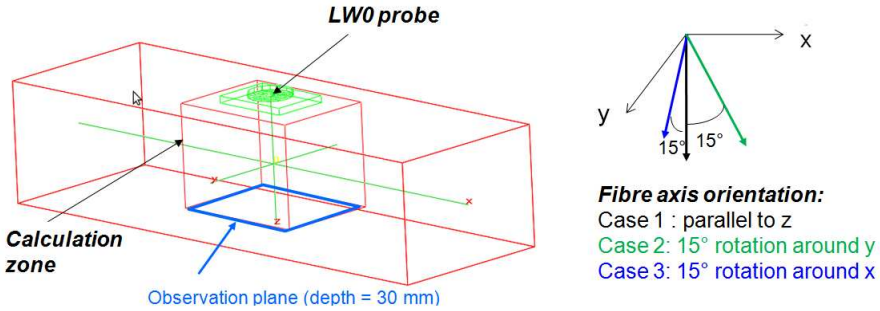

Figure 11. Computation configuration for the 3 orientations of the symmetry axis (Fiber orientation) of the medium

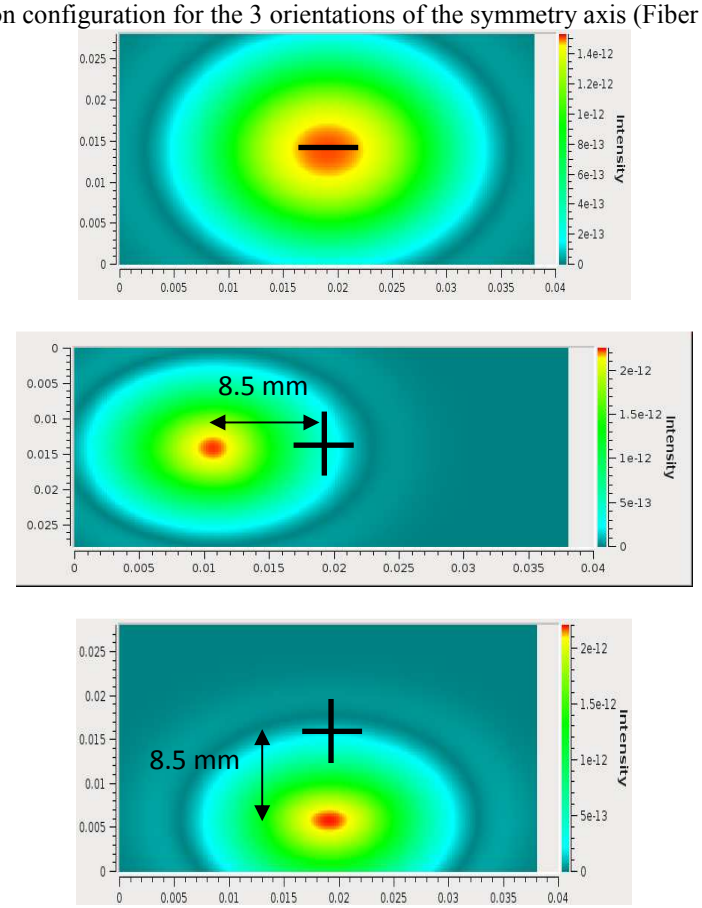

Figure 12. sound field calculated at the observation plane using ATHENA 3D when the symmetry axis is a) parallel to z, b) rotated around the y axis and c) rotated around the x axis

10. Conclusion

In the present paper, the new version of the ATHENA code is presented. It allows 3D finite element calculation and is optimized for parallelized computation. Consequently, in numerous configurations, the use of such a code is no more prohibitively time consuming when launching the computation on a calculation cluster.

Furthermore, the first validations cases detailed in this work showed that the ATHENA code was able to reproduce both wave propagation and wave to defect interaction in isotropic and homogeneous media. In addition, various kinds of ultrasonic probes (single and multi-element probes, immersion, contact, plane wave, focalized wave, etc.) can be handled by ATHENA through the use of its GUI MILENAQt.

However, this validation work must be continued. Indeed, simulation of Distance-Amplitude Curve (DAC) covering a wide range of depth is needed in order to quantitatively define the validation domain of the code. Furthermore, in this study, the comparison between the sound fields obtained from CIVA 10 and ATHENA 3D was only based on the determination of the focal depth. Consequently, a more exhaustive comparison of the sound fields providing by each code should be of great interest.

Finally, even if a preliminary result obtained in an anisotropic homogeneous medium has been shown in this paper, it is necessary to perform simulation on heterogeneous structures such as austenitic welds.

References

[1] Chassignole B, Villard D, Dubuget M, Baboux J-C and El Guerjouma R 2000 Characterization of austenitic stainless steel welds for ultrasonic NDT *Review of Progress in QNDE* **19** AIP Conference Proceedings, **509**, 1325-32

[2] Feuilly N, Dupond O, Chassignole B, Moysan J and Comeloup G 2009 Relation between ultrasonic backscattering and microstructure for polycrystalline materials *Review of Progress in QNDE* **28** AIP Conference Proceedings, **1096**, 1216-23

[3] Rupin F, Blatman G, Lacaze S and Fouquet T 2013 Sensitivity analysis of an ultrasonic inspection of a weld structure simulated with the finite element code ATHENA 2D *Review of Progress in QNDE* AIP Conference Proceedings, **1511**, 1089-96

[4] Chassignole B, Duwig V, Ploix M-A, Guy P and El Guerjouma R 2009 Modelling the attenuation in the ATHENA finite elements code for the ultrasonic testing of austenitic stainless steel welds *Ultrasonics* **49** 653-8

[5] Chassignole B, El Guerjouma R, Ploix M-A, Fouquet T 2010 Ultrasonic and structural characterization of anisotropic austenitic stainless steel welds: Towards a higher reliability in ultrasonic non-destructive testing *NDT&E Int*. **43** 273-82

[6] Chassignole B, Dupond O, Doudet L, Duwig V and Etchegaray N 2009 Ultrasonic examination of an austenitic weld: illustration of the disturbances of the ultrasonic beam *Review of Progress in QNDE* **28**, AIP Conference Proceedings, **1096**, 1886-93

[7] Hannemann R, Marklein R, Langenberg K J, Schurig C, Köhler B and Walte F 2000 Ultrasonic wave propagation in real-life austenitic V-Butt welds: numerical modeling and validation*Review of Progress in QNDE* **19** AIP Conference Proceedings **509**, 145-52

[8] Apfel A, Moysan J, Corneloup G, Fouquet T and Chassignole B 2005 Coupling an ultrasonic propagation code with a model of the heterogeneity of multipass welds to simulate ultrasonic testing *Ultrasonics* **43** 447-56

[9] Chassignole B, Diaz J, Duwig V, Fouquet T and Schumm A 2006 Structural noise in modelisation *in ECNDT 2006 proceedings* Fr.1.4.4, 1-13

[10] Shahjahana S, Rupin F, Fouquet T, Aubryc A and Derode A 2012 Structural noise and coherent backscattering modelled with the ATHENA2D finite element code *in Acoustics 2012*, Nantes, 2639-44

[11] Bécache E, Joly P and Tsogka C 2001 Fictitious domains, mixed finite elements and perfectly matched layers for 2D elastic wave propagation *J. Comp. Acoustics* **9** 1175-201

[12] Bécache E, Joly P and Tsogka C 2000 An analysis of new mixed finite elements for the approximation of wave propagation problems *SIAM J. Num. Anal.* **37**, 1053-84

Acknowledgement

This work was realized in the framework of the MOSAICS project (Modeling of an austenitic stainless steel weld inspected by ultrasonic techniques) which is supported by the French National Agency of Research.